

Two-flavor lattice QCD simulation in the ϵ -regime with exact chiral symmetry

H. Fukaya,¹ S. Aoki,^{2,3} T.W. Chiu,⁴ S. Hashimoto,^{5,6} T. Kaneko,^{5,6}
 H. Matsufuru,⁵ J. Noaki,⁵ K. Ogawa,⁴ M. Okamoto,⁵ T. Onogi,⁷ and N. Yamada^{5,6}

(JLQCD collaboration)

¹ *Theoretical Physics Laboratory, RIKEN, Wako 351-0198, Japan*

² *Graduate School of Pure and Applied Sciences,
 University of Tsukuba, Tsukuba 305-8571, Japan*

³ *Riken BNL Research Center, Brookhaven National Laboratory, Upton, NY11973, USA*

⁴ *Physics Department and Center for Theoretical Sciences,
 National Taiwan University, Taipei, 10617, Taiwan*

⁵ *High Energy Accelerator Research Organization (KEK), Tsukuba 305-0801, Japan*

⁶ *School of High Energy Accelerator Science, The Graduate University
 for Advanced Studies (Sokendai), Tsukuba 305-0801, Japan*

⁷ *Yukawa Institute for Theoretical Physics, Kyoto University, Kyoto 606-8502, Japan*

Abstract

We perform lattice simulations of two-flavor QCD using Neuberger's overlap fermion, with which the exact chiral symmetry is realized at finite lattice spacings. The ϵ -regime is reached by decreasing the light quark mass down to 3 MeV on a $16^3 \times 32$ lattice with a lattice spacing ~ 0.11 fm. We find a good agreement of the low-lying Dirac eigenvalue spectrum with the analytical predictions of the chiral random matrix theory, which reduces to the chiral perturbation theory in the ϵ -regime. The chiral condensate is extracted as $\Sigma^{\overline{\text{MS}}}(2 \text{ GeV}) = (251 \pm 7 \pm 11 \text{ MeV})^3$, where the errors are statistical and an estimate of the higher order effects in the ϵ -expansion.

In Quantum Chromodynamics (QCD), it is widely believed that chiral symmetry is spontaneously broken, making pions nearly massless while giving masses of order Λ_{QCD} , the QCD scale, to the other hadrons. In fact, the Chiral Perturbation Theory (ChPT), an effective theory based on the spontaneously broken chiral symmetry, describes low energy interactions of pions very accurately. Nevertheless, theorists have not been successful in analytically solving QCD and deriving the chiral symmetry breaking, due to its highly non-perturbative dynamics.

The most promising approach to establishing the link between QCD and ChPT is to utilize the numerical simulation of lattice QCD, with which the every prediction of ChPT can be tested in principle. For instance, the presence of the so-called chiral logarithms, the effect of pion cloud, should be reproduced. Such a numerical test is, however, not an easy task, because of rapidly increasing computational cost in the small quark mass region where ChPT is reliably applied. Another serious problem is the explicit violation of the chiral symmetry at finite lattice spacings in the conventional fermion formulations, with which the conclusive test of ChPT requires well-controlled and thus computationally demanding continuum extrapolation.

In this work we improve this situation in two ways. First, we employ Neuberger's overlap fermion [1, 2] for dynamical quarks. It preserves exact chiral symmetry at finite lattice spacings, and hence ChPT can be applied before taking the continuum limit. Although the numerical cost of the overlap fermion is almost 100 times higher than that of the other fermions, new computational facilities at KEK enable us to carry out such a work.

Second, we study the correspondence between QCD and ChPT in the so-called ϵ -regime [3, 4, 5], which is characterized by the small pion mass m_π satisfying $m_\pi L \lesssim 1$ with L the box size. In this regime ChPT is safely applied as an expansion in terms of $\epsilon^2 \sim m_\pi/\Lambda_{\text{QCD}}$, provided that the condition $1/(\Lambda_{\text{QCD}}L)^2 \ll 1$, the usual condition that the box size is larger than the inverse QCD scale, is satisfied. We set the sea quark mass to ~ 3 MeV, for which $m_\pi L \simeq 1.0$. With the space-time volume $L^3 \times T \simeq (1.8 \text{ fm})^3 \times (3.5 \text{ fm})$, the numerical cost is still not prohibitive even with such a small sea quark mass, since the finite volume provides a natural lower bound on the lowest eigenvalue of the Dirac operator.

In the ϵ -regime, zero-momentum modes of the pion field dominate the dynamics and the kinetic term gives only subleading contributions. The Lagrangian of ChPT reduces to $\mathcal{L}^{(0)} = m\Sigma \text{ReTr}[U]$ with m the (degenerate) quark mass and U ($\in \text{SU}(N_f)$) the pion field

($N_f = 2$ in this work). The system is fully characterized by a parameter $m\Sigma V$, where Σ is the chiral condensate and V is the space-time volume $L^3 \times T$. Dependence on the topological charge Q of the gauge field also becomes significant.

At the leading order of the ϵ -expansion, the chiral Random Matrix Theory (ChRMT) provides an equivalent description of ChPT [6, 7, 8]. Furthermore, ChRMT can predict the distributions of the individual eigenvalues of the Dirac operator, which may be directly compared with the lattice data. In the quenched approximation, a good agreement between ChRMT and lattice calculation has been observed using the overlap-Dirac operator [9, 10, 11], and Σ has been determined by matching the eigenvalues [12]. The present work is an extension of these works to two-flavor QCD. A preliminary report of this work has been presented in [13], and an overview of our dynamical overlap fermion project is found in [14]. Similar studies have been done recently [15, 16], but the ϵ -regime was not reached because of larger sea quark masses.

We have performed numerical simulations on a $16^3 \times 32$ lattice at a lattice spacing $a \sim 0.11$ fm as determined from the scale $r_0 (=0.49\text{fm})$ of the heavy quark potential. We employ the overlap fermion [1, 2], whose Dirac operator is

$$D(m) = \left(m_0 + \frac{m}{2}\right) + \left(m_0 - \frac{m}{2}\right) \gamma_5 \text{sgn}[H_W(-m_0)] \quad (1)$$

for the quark mass m . Here, $H_W(-m_0)$ denotes the standard hermitian Wilson-Dirac operator $H_W(-m_0) \equiv \gamma_5 D_W(-m_0)$ with a large negative mass term (we choose $m_0 = 1.6$ throughout this work). For the gauge part, the Iwasaki action is used at $\beta = 2.35$ together with unphysical Wilson fermions and associated twisted-mass ghosts [17], which preserves the global topological charge during molecular-dynamics evolutions of the gauge field. This is desirable for the ϵ -regime simulations since we can effectively accumulate statistics at a given topological charge. In this work our simulation is confined in a topological sector $Q = 0$.

For the simulation with the dynamical overlap fermions [18], we use the Hybrid Monte Carlo (HMC) algorithm. The sign function in (1) is approximated by a rational function with Zolotarev's optimal coefficients after projecting out low-lying eigenvalues of $|H_W(-m_0)|$. With 10 poles the sign function has a $10^{-(7-8)}$ precision. Thanks to the extra Wilson fermions, the lowest eigenvalue of $H_W(-m_0)$ never passes zero, and hence no special care of the discontinuity of the fermion determinant is needed.

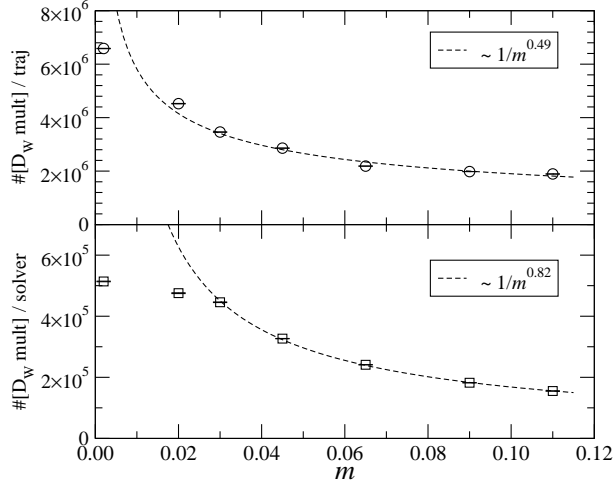


FIG. 1: Number of the Wilson-Dirac operator multiplication per trajectory (upper panel) and per an overlap inversion (lower panel). The curves are fit to data above $m = 0.030$ with the form $\propto 1/m^\alpha$.

The simulation cost is substantially reduced by the mass preconditioning of the HMC Hamiltonian [20]. The heavier overlap fermion mass for the preconditioner is chosen to 0.4 except for two lightest sea quark masses where the value is 0.2. The relaxed conjugate gradient algorithm to invert the overlap-Dirac operator [19] also helps to speed up the simulation by about a factor of 2.

For the sea quark mass we take seven values: 0.110, 0.090, 0.065, 0.045, 0.030, 0.020, and 0.002. The lightest sea quark ($m = 0.002$) corresponds to the ϵ -regime. The simulation cost measured by the number of the Wilson-Dirac operator multiplication is plotted in Fig. 1. The upper panel shows the cost per trajectory of length 0.5; the lower panel presents the cost of inverting the overlap-Dirac operator when we calculate the Hamiltonian at the end of each trajectory. Increase of the numerical cost towards the chiral limit is not as strong as expected: if we fit the data assuming the scaling law $\sim 1/m^\alpha$ above $m = 0.030$, the power α is 0.82 for the inversion and 0.49 for the total cost. In the ϵ -regime the cost is even lower than the expectation from the power law. This is because the cost is governed by the lowest-lying eigenvalue rather than the quark mass as explained below.

The number of trajectories is 1,100 for each sea quark mass after discarding 500 for thermalization. For the ϵ -regime run at $m = 0.002$, we have accumulated 4,600 trajectories. In addition, we have generated quenched lattices at a similar lattice spacing with $Q = 0$ and

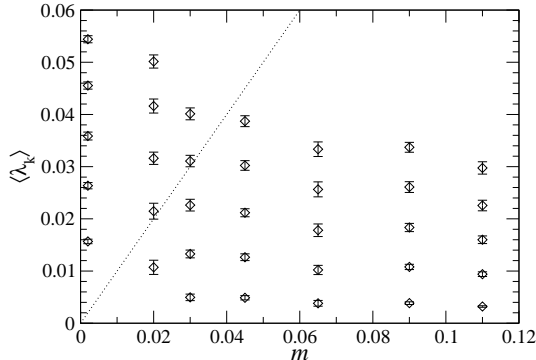


FIG. 2: Lowest 5 eigenvalues λ_k as a function of sea quark mass. Dashed line shows $\lambda = m$.

2. The computational cost at $m = 0.002$ is about one hour per trajectory on a half rack (512 nodes) of the IBM BlueGene/L (2.8 TFlops peak performance).

The lowest 50 eigenvalues of the overlap-Dirac operator $D(0)$ are calculated at every 10 trajectories. We use the implicitly restarted Lanczos algorithm for a chirally projected operator $P_+ D(0) P_+$, where $P_+ = (1 + \gamma_5)/2$. From its eigenvalue $\text{Re}\lambda^{ov}$ the pair of eigenvalues λ^{ov} (and its complex conjugate) of $D(0)$ is extracted through the relation $|1 - \lambda^{ov}/m_0|^2 = 1$, that forms a circle on a complex plane. For the comparison with ChRMT, the lattice eigenvalue λ^{ov} is projected onto the imaginary axis as $\lambda \equiv \text{Im}\lambda^{ov}/(1 - \text{Re}\lambda^{ov}/(2m_0))$. Note that λ is very close to $\text{Im}\lambda^{ov}$ (within 0.05%) for the low-lying modes we are interested in.

In Fig. 2 we plot the ensemble averages of the lowest 5 eigenvalues $\langle \lambda_k \rangle$ ($k = 1-5$) as a function of the sea quark mass. We observe that the low-lying spectrum is lifted as the chiral limit is approached. This is a direct consequence of the fermion determinant $\sim \prod_k (|\lambda_k|^2 + m^2)$, which repels the small eigenvalues from zero when m becomes smaller than the lowest eigenvalue. This is exactly the region where the numerical cost saturates as it is controlled by λ_1 rather than m . We also find that the autocorrelation length of the lowest eigenvalues is significantly longer in the ϵ -regime. We therefore use the jackknife method in the statistical analysis with a bin size of 200 trajectories, with which the statistical error saturates.

In the ϵ -regime, ChRMT predicts the probability distribution $p_k(\zeta_k)$ of lowest-lying eigenvalues ζ_k , and thus their ensemble averages $\langle \zeta_k \rangle = \int_0^\infty d\zeta_k \zeta_k p_k(\zeta_k)$. The correspondence between ChRMT and ChPT implies the relation $\langle \zeta_k \rangle = \langle \lambda_k \rangle \Sigma V$, from which we can extract Σ , once $\langle \lambda_k \rangle$'s are obtained. Correction for finite sea quark mass m can also be calculated by ChRMT. At $m = 0.002$, it is only 0.9% for the lowest eigenvalue, which is taken into

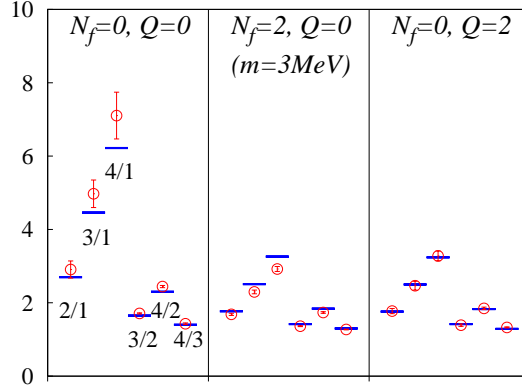


FIG. 3: Ratio of the eigenvalues $\langle \zeta_k \rangle / \langle \zeta_l \rangle$ for combinations of k and $l \in 1-4$ (denoted in the plot as k/l). In addition to the two-flavor QCD data (middle), quenched data at $Q = 0$ (left) and 2 (right) are also shown. Lattice data (circles) are compared with the ChRMT predictions (bars).

account in the following analysis.

We first compare the pattern of the eigenvalue spectrum of the Dirac operator. In the ratios $\langle \zeta_k \rangle / \langle \zeta_l \rangle$ of low-lying eigenvalues the factor ΣV drops off and the comparison is parameter free. As Fig. 3 shows, the lattice data agree well with the ChRMT predictions (middle panel). It is also known that there exists the so-called flavor-topology duality in ChRMT: the low-mode spectrum is identical between the two-flavor (massless) theory at $Q = 0$ and the quenched theory at $Q = 2$ (right panel), while the quenched spectrum at $Q = 0$ is drastically different (left panel). This is nicely reproduced by the lattice data. These clear patterns indicate that the low-lying modes of the QCD Dirac operator are in fact responsible for the zero-momentum mode of the pion field U , which induce the vacuum with spontaneously broken chiral symmetry.

If we look into the details, however, there is a slight disagreement in higher eigenvalues. For instance, the deviation in the combination $k/l = 4/1$ is 10%. The reason for this will be discussed later.

Another non-trivial comparison can be made through the shape of the eigenvalue distributions. We plot the cumulative distribution $c_k(\zeta_k) \equiv \int_0^{\zeta_k} d\zeta' p_k(\zeta')$ of the three lowest eigenvalues in Fig. 4. The agreement between the lattice data and ChRMT (solid curves) is quite good for the lowest eigenvalue. For the higher modes the agreement of the central value is marginal while the shape seems well described by ChRMT. Table I lists the numer-

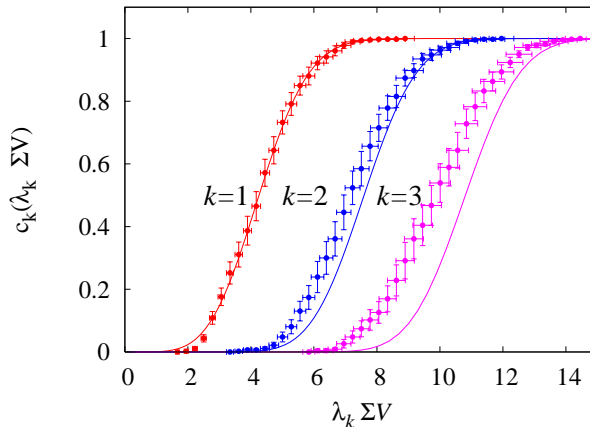


FIG. 4: Cumulative distribution of the low-lying eigenvalues. The horizontal error comes from the statistical error of Σ . The solid curves are the ChRMT results with the input from the average $\langle \lambda_1 \rangle$.

	$\langle \zeta_k \rangle$	$\langle \lambda_k \rangle \Sigma V$	$\langle \Delta \zeta_k \rangle$	$\langle \Delta \lambda_k \rangle \Sigma V$
$k = 1$	4.30	[4.30]	1.234	1.215(48)
$k = 2$	7.62	7.25(13)	1.316	1.453(83)
$k = 3$	10.83	9.88(21)	1.373	1.587(97)
$k = 4$	14.01	12.58(28)	1.414	1.54(10)

TABLE I: Comparison of the low-mode spectrum of ChRMT and the lattice data. The number given in $[]$ is used as an input.

ical results of both ChRMT and lattice data. To characterize the shape of the distribution, we define the width $\langle \Delta \zeta_k \rangle \equiv \sqrt{\langle \zeta_k^2 \rangle - \langle \zeta_k \rangle^2}$ as well as its lattice counterpart $\langle \Delta \lambda_k \rangle \Sigma V$. The overall agreement is very good, but we see deviations of about 10% in the averages and 16% in the widths, at the largest.

Because of the exact chiral symmetry in our simulation, we do not expect significant effects due to finite a in the comparison of low-lying eigenvalues. The largest possible source of systematic errors is the higher order effects in the ϵ -expansion, which is a finite volume effect. Although the higher order corrections can not be calculated within the framework of ChRMT, an estimate of their size can be given by ChPT. The next-to-leading order correction to the chiral condensate is given by $\Sigma[1 + ((N_f^2 - 1)/N_f)\beta_1/(FL)^2]$, where β_1 is a numerical constant depending on the lattice geometry [3]. Numerically, the correction is

13% (we assume the pion decay constant $F = 93$ MeV), which is about the same size of the deviation of the eigenvalue distributions.

Since the contribution from finite momentum modes is expected to be more significant for higher eigenvalues, we take the lowest eigenvalue as an input for the determination of Σ . From the average of λ_1 we obtain $\Sigma^{lat} a^3 = 0.00212(6)$ in the lattice unit and $\Sigma^{lat} = [240(2)(6) \text{ MeV}]^3$ in the physical unit. The second error in the latter comes from the lattice scale $a = 0.107(3)$ fm. We put a superscript *lat* in order to emphasize that it is defined on the lattice.

In order to convert Σ^{lat} to the definition in the $\overline{\text{MS}}$ scheme, we have calculated the renormalization factor $Z_S^{\overline{\text{MS}}}(2 \text{ GeV})$ using the non-perturbative renormalization technique through the RI/MOM scheme [21]. Calculation is done at $m = 0.002$ with several different valence quark masses. The result is $Z_S^{\overline{\text{MS}}}(2 \text{ GeV}) = 1.14(2)$. Details of this calculation will be presented elsewhere.

Including the renormalization factor, our final result is $\Sigma^{\overline{\text{MS}}}(2 \text{ GeV}) = [251(7)(11) \text{ MeV}]^3$. The errors represent a combined statistical error (from λ_1 , r_0 and $Z_S^{\overline{\text{MS}}}$) and the systematic error estimated from the higher order effects in the ϵ -expansion, respectively. Since the calculation is done at a single lattice spacing, the discretization error cannot be quantified reliably, but we do not expect much larger error because our lattice action is free from $O(a)$ discretization effects.

In this letter we demonstrated that the lattice QCD simulation is feasible near the chiral limit, as far as the exact chiral symmetry is respected. The link between QCD and ChPT is established in the ϵ -regime without recourse to chiral extrapolations. From their correspondence, the low energy constants, such as the chiral condensate, can be precisely calculated. Improvement of the precision may be achieved by increasing the physical volume, as the higher order effects in the ϵ -expansion are suppressed as $1/L^2$. Further information on the low energy constants can be extracted in the ϵ -regime by calculating two- and three-point functions or analyzing the Dirac eigenvalue spectrum with imaginary chemical potential [22, 23, 24]. This work is a first step towards such programs.

Acknowledgments

We thank P.H. Damgaard and S.M. Nishigaki for fruitful discussions at the YITP workshop YITP-W-05-25 on “Actions and Symmetries in Lattice Gauge Theory.” Numerical simulations are performed on IBM System Blue Gene Solution at High Energy Accelerator Research Organization (KEK) under a support of its Large Scale Simulation Program (No. 06-13). This work is supported in part by the Grant-in-Aid of the Japanese Ministry of Education (No. 13135204, 1315213, 15540251, 16740156, 17740171, 18340075, 18034011, 18740167, and 18840045) and the National Science Council of Taiwan (No. NSC95-2112-M002-005).

-
- [1] H. Neuberger, Phys. Lett. B **417**, 141 (1998) [arXiv:hep-lat/9707022].
 - [2] H. Neuberger, Phys. Lett. B **427**, 353 (1998) [arXiv:hep-lat/9801031].
 - [3] J. Gasser and H. Leutwyler, Phys. Lett. B **188**, 477 (1987).
 - [4] F. C. Hansen, Nucl. Phys. B **345**, 685 (1990).
 - [5] F. C. Hansen and H. Leutwyler, Nucl. Phys. B **350**, 201 (1991).
 - [6] E. V. Shuryak and J. J. M. Verbaarschot, Nucl. Phys. A **560**, 306 (1993) [arXiv:hep-th/9212088].
 - [7] J. J. M. Verbaarschot and I. Zahed, Phys. Rev. Lett. **70**, 3852 (1993) [arXiv:hep-th/9303012].
 - [8] P. H. Damgaard and S. M. Nishigaki, Phys. Rev. D **63**, 045012 (2001) [arXiv:hep-th/0006111].
 - [9] R. G. Edwards, U. M. Heller, J. E. Kiskis and R. Narayanan, Phys. Rev. Lett. **82**, 4188 (1999) [arXiv:hep-th/9902117].
 - [10] W. Bietenholz, K. Jansen and S. Shcheredin, JHEP **0307**, 033 (2003) [arXiv:hep-lat/0306022].
 - [11] L. Giusti, M. Luscher, P. Weisz and H. Wittig, JHEP **0311**, 023 (2003) [arXiv:hep-lat/0309189].
 - [12] J. Wennekers and H. Wittig, JHEP **0509**, 059 (2005) [arXiv:hep-lat/0507026].
 - [13] H. Fukaya *et al.* [JLQCD Collaboration], arXiv:hep-lat/0610024.
 - [14] T. Kaneko *et al.* [JLQCD Collaboration], arXiv:hep-lat/0610036.
 - [15] T. DeGrand, Z. Liu and S. Schaefer, Phys. Rev. D **74**, 094504 (2006) [Erratum-ibid. D **74**, 099904 (2006)] [arXiv:hep-lat/0608019].

- [16] C. B. Lang, P. Majumdar and W. Ortner, arXiv:hep-lat/0611010.
- [17] H. Fukaya, S. Hashimoto, K. I. Ishikawa, T. Kaneko, H. Matsufuru, T. Onogi and N. Yamada [JLQCD Collaboration], Phys. Rev. D **74**, 094505 (2006) [arXiv:hep-lat/0607020].
- [18] Z. Fodor, S. D. Katz and K. K. Szabo, JHEP **0408**, 003 (2004) [arXiv:hep-lat/0311010].
- [19] N. Cundy, J. van den Eshof, A. Frommer, S. Krieg, T. Lippert and K. Schafer, Comput. Phys. Commun. **165**, 221 (2005) [arXiv:hep-lat/0405003].
- [20] M. Hasenbusch, Phys. Lett. B **519**, 177 (2001) [arXiv:hep-lat/0107019].
- [21] G. Martinelli, C. Pittori, C. T. Sachrajda, M. Testa and A. Vladikas, Nucl. Phys. B **445**, 81 (1995) [arXiv:hep-lat/9411010].
- [22] P. H. Damgaard, M. C. Diamantini, P. Hernandez and K. Jansen, Nucl. Phys. B **629**, 445 (2002) [arXiv:hep-lat/0112016].
- [23] P. Hernandez and M. Laine, JHEP **0610**, 069 (2006) [arXiv:hep-lat/0607027].
- [24] G. Akemann, P. H. Damgaard, J. C. Osborn and K. Splittorff, arXiv:hep-th/0609059.